

Study of the heavy CP-even Higgs with mass 125 GeV in two-Higgs-doublet models at the LHC and ILC

Lei Wang, Xiao-Fang Han

Department of Physics, Yantai University, Yantai 264005, PR China

Abstract

We assume that the 125 GeV Higgs discovered at the LHC is the heavy CP-even Higgs of the two-Higgs-doublet models, and examine the parameter space in the Type-I, Type-II, Lepton-specific and Flipped models allowed by the latest Higgs signal data, the relevant experimental and theoretical constraints. Further, we show the projected limits on $\tan\beta$, $\sin(\beta - \alpha)$, $Hf\bar{f}$ and HVV couplings from the future measurements of the 125 GeV Higgs at the LHC and ILC, including the LHC with integrated luminosity of 300 fb^{-1} (LHC-300 fb^{-1}) and 3000 fb^{-1} (LHC-3000 fb^{-1}) as well as the ILC at $\sqrt{s} = 250 \text{ GeV}$ (ILC-250 GeV), $\sqrt{s} = 500 \text{ GeV}$ (ILC-500 GeV) and $\sqrt{s} = 1000 \text{ GeV}$ (ILC-1000 GeV). Assuming that the future Higgs signal data have no deviation from the SM expectation, the LHC-300 fb^{-1} , LHC-3000 fb^{-1} and ILC-1000 GeV can exclude the wrong-sign Yukawa coupling regions of the Type-II, Flipped and Lepton-specific models at the 2σ level, respectively. The future experiments at the LHC and ILC will constrain the Higgs couplings to be very close to SM values, especially for the HVV coupling.

PACS numbers: 12.60.Fr, 14.80.Ec, 14.80.Bn

I. INTRODUCTION

The ATLAS and CMS collaborations have announced the observation of a scalar [1, 2], which is supported by the Tevatron search [3]. The properties of this particle with large experimental uncertainties are well consistent with the SM Higgs boson, which can give the strong constraints on the new physics models.

The two-Higgs-doublet model (2HDM) has very rich Higgs phenomenology, including two neutral CP-even Higgs bosons h and H , one neutral pseudoscalar A , and two charged Higgs H^\pm . The observed signal strengths of the Higgs boson can give the strong constraints on the 2HDMs. The 2HDMs generically have tree-level flavor changing neutral currents (FCNC), which can be forbidden by a discrete symmetry. There are four traditional types for 2HDMs, which are typically called the Type-I [4, 5], Type-II [4, 6], Lepton-specific, and Flipped models [7–12] according to their different Yukawa couplings. In addition, there is no tree-level FCNC in the 2HDM that allows both doublets to couple to the fermions with aligned Yukawa matrices (A2HDM) [13]. In light of the recent Higgs data, there have been various studies on these 2HDMs over the last few months [14–36].

In this paper, we assume that the 125 GeV Higgs discovered at the LHC is respectively the heavy CP-even Higgs of the Type-I, Type-II, Lepton-specific and Flipped 2HDMs, and examine the parameter space allowed by the latest Higgs signal data (up to March 2014), the non-observation of additional Higgs at the collider, and the theoretical constraints from vacuum stability, unitarity and perturbativity as well as the experimental constraints from the electroweak precision data and flavor observables. Further, we analyze how well 2HDMs can be distinguished from the SM by the future measurements of the 125 GeV Higgs at the LHC and ILC, including the LHC with the center of mass energy $\sqrt{s} = 14$ TeV and integrated luminosity of 300 fb^{-1} (LHC-300 fb^{-1}) and 3000 fb^{-1} (LHC-3000 fb^{-1}) as well as the ILC at $\sqrt{s} = 250$ GeV (ILC-250 GeV), $\sqrt{s} = 500$ GeV (ILC-500 GeV) and $\sqrt{s} = 1000$ GeV (ILC-1000 GeV). For the 125 GeV Higgs is the light CP-even Higgs, the projected limits on 2HDMs from the future measurements of the 125 GeV Higgs at the LHC and ILC have been studied in [26, 27].

Our work is organized as follows. In Sec. II we recapitulate the two-Higgs-doublet models. In Sec. III we introduce the numerical calculations. In Sec. IV, we examine the implications of the latest Higgs signal data on the 2HDMs and projected limits on the 2HDMs from

the future measurements of the 125 GeV Higgs at the LHC and ILC after imposing the theoretical and experimental constraints. Finally, we give our conclusion in Sec. V.

II. TWO-HIGGS-DOUBLET MODELS

The general Higgs potential is written as [37]

$$\begin{aligned}
V = & m_{11}^2(\Phi_1^\dagger\Phi_1) + m_{22}^2(\Phi_2^\dagger\Phi_2) - \left[m_{12}^2(\Phi_1^\dagger\Phi_2 + \text{h.c.}) \right] \\
& + \frac{\lambda_1}{2}(\Phi_1^\dagger\Phi_1)^2 + \frac{\lambda_2}{2}(\Phi_2^\dagger\Phi_2)^2 + \lambda_3(\Phi_1^\dagger\Phi_1)(\Phi_2^\dagger\Phi_2) + \lambda_4(\Phi_1^\dagger\Phi_2)(\Phi_2^\dagger\Phi_1) \\
& + \left[\frac{\lambda_5}{2}(\Phi_1^\dagger\Phi_2)^2 + \text{h.c.} \right] + \left[\lambda_6(\Phi_1^\dagger\Phi_1)(\Phi_1^\dagger\Phi_2) + \text{h.c.} \right] \\
& + \left[\lambda_7(\Phi_2^\dagger\Phi_2)(\Phi_1^\dagger\Phi_2) + \text{h.c.} \right].
\end{aligned} \tag{1}$$

We impose a discrete Z_2 symmetry on the Lagrangian, which leads to $\lambda_6 = \lambda_7 = 0$. $m_{12}^2 \neq 0$ is still allowed as a "soft" breaking of the Z_2 symmetry. We focus on the CP-conserving model in which all λ_i and m_{12}^2 are real. The two complex scalar doublets have the hypercharge $Y = 1$,

$$\Phi_1 = \begin{pmatrix} \phi_1^+ \\ \frac{1}{\sqrt{2}}(v_1 + \phi_1^0 + ia_1) \end{pmatrix}, \quad \Phi_2 = \begin{pmatrix} \phi_2^+ \\ \frac{1}{\sqrt{2}}(v_2 + \phi_2^0 + ia_2) \end{pmatrix}. \tag{2}$$

Where v_1 and v_2 are the electroweak vacuum expectation values (VEVs) with $v^2 = v_1^2 + v_2^2 = (246 \text{ GeV})^2$. The ratio of the two VEVs is defined as usual to be $\tan\beta = v_2/v_1$. After spontaneous electroweak symmetry breaking, the physical scalars are two neutral CP-even h and H , one neutral pseudoscalar A , and two charged scalar H^\pm .

The tree-level couplings of the neutral Higgs bosons can have sizable deviations from those of SM Higgs boson. Table I shows the couplings of the heavy CP-even Higgs with respect to those of the SM Higgs boson in the Type-I, Type-II, Lepton-specific and Flipped models.

III. NUMERICAL CALCULATIONS

We use HiggsSignals-1.2.0 [38] to perform a global χ^2 fit to the most up-to-date Higgs signal data at the LHC and Tevatron as of March 2014, which includes 80 Higgs signal strengths observables from ATLAS [39–46], CMS [47–58], CDF [59] and D0 [60] collaborations as well as the four Higgs mass measurements from the ATLAS and CMS $h \rightarrow \gamma\gamma$ and

TABLE I: The tree-level couplings of the heavy CP-even Higgs with respect to those of the SM Higgs boson. u , d and l denote the up-type quarks, down-type quarks and the charged leptons, respectively.

model	HVV (WW , ZZ)	$Hu\bar{u}$	$Hd\bar{d}$	$Hl\bar{l}$
Type-I	$\cos(\beta - \alpha)$	$\frac{\sin \alpha}{\sin \beta}$	$\frac{\sin \alpha}{\sin \beta}$	$\frac{\sin \alpha}{\sin \beta}$
Type-II	$\cos(\beta - \alpha)$	$\frac{\sin \alpha}{\sin \beta}$	$\frac{\cos \alpha}{\cos \beta}$	$\frac{\cos \alpha}{\cos \beta}$
Lepton-specific	$\cos(\beta - \alpha)$	$\frac{\sin \alpha}{\sin \beta}$	$\frac{\sin \alpha}{\sin \beta}$	$\frac{\cos \alpha}{\cos \beta}$
Flipped	$\cos(\beta - \alpha)$	$\frac{\sin \alpha}{\sin \beta}$	$\frac{\cos \alpha}{\cos \beta}$	$\frac{\sin \alpha}{\sin \beta}$

$h \rightarrow ZZ^* \rightarrow 4l$ analyses. These experimental data are listed in the [61]. For the detailed introduction on the calculation of χ^2 in **HiggsSignals-1.2.0**, see [38, 61]. In our discussions, we will pay particular attention to the surviving samples with $\chi^2 - \chi^2_{\min} \leq 6.18$, where χ^2_{\min} denotes the minimum of χ^2 . These samples correspond to the 95.4% confidence level regions in any two dimensional plane of the model parameters when explaining the Higgs data (corresponding to be within 2σ range).

We employ **2HDMC-1.6.4** [62] to implement the theoretical constraints from the vacuum stability, unitarity and coupling-constant perturbativity. Also the oblique parameters (S , T , U) and $\delta\rho$ are calculated and the corresponding experimental data are from [63]. $\delta\rho$ has been measured very precisely via Z-pole precision observables to be very close to 1, which imposes a strong constraint on the mass difference between the various Higgses in 2HDMs. **SuperIso-3.3** [64] is used to implement the constraints from flavor observables, including $B \rightarrow X_s \gamma$ [65], $B_s \rightarrow \mu^+ \mu^-$ [66], $B_u \rightarrow \tau \nu$ [67] and $D_s \rightarrow \tau \nu$ [65]. **HiggsBounds-4.1.0** [68, 69] is used to implement the exclusion constraints from the neutral and charged Higgses searches at LEP, Tevatron and LHC at 95% confidence level. The constrains from Δm_{B_d} [70] and Δm_{B_s} [70] are considered, which are calculated using the formulas in [71]. In addition, R_b is calculated by

$$R_b \equiv (1 + \frac{S_b^{SM}}{s_b^{SM} + \delta s_b} C_b)^{-1} = R_b^{SM} (1 + \frac{\delta s_b}{s_b^{SM}}) / (1 + R_b^{SM} \frac{\delta s_b}{s_b^{SM}}), \quad (3)$$

where

$$s_b^{SM} = [(\bar{g}_b^L - \bar{g}_b^R)^2 + (\bar{g}_b^L + \bar{g}_b^R)^2] (1 + \frac{3\alpha}{4\pi} Q_b^2), \quad \delta s_b = s_b - s_b^{SM}. \quad (4)$$

We take the SM value $R_b^{SM} = 0.21550 \pm 0.00003$ [72] and the experimental data $R_b^{exp} =$

TABLE II: Projected 1σ sensitivities of channels for the LHC operating $\sqrt{s} = 14$ TeV. The 300 fb^{-1} and 3000 fb^{-1} sensitivities are taken from Ref. [76] for ATLAS and Ref. [77] for CMS. The assumed signal composition is taken from Ref. [61]

Channel	Projected 1σ sensitivity		Assumed signal composition (%)				
	300 fb^{-1}	3000 fb^{-1}	ggH	VBF	WH	ZH	$t\bar{t}H$
ATL (pp) $\rightarrow h \rightarrow \gamma\gamma$ (0jet)	0.22	0.20	91.6	2.7	3.2	1.8	0.6
ATL (pp) $\rightarrow h \rightarrow \gamma\gamma$ (1jet)	0.37	0.37	81.8	13.2	2.9	1.6	0.5
ATL (pp) $\rightarrow h \rightarrow \gamma\gamma$ (VBF-like)	0.47	0.21	39.2	58.4	1.4	0.8	0.3
ATL (pp) $\rightarrow h \rightarrow \gamma\gamma$ (VH -like)	0.77	0.26	2.5	0.4	63.3	15.2	18.7
ATL (pp) $\rightarrow h \rightarrow \gamma\gamma$ ($t\bar{t}H$ -like)	0.55	0.21	0.0	0.0	0.0	0.0	100.0
ATL (pp) $\rightarrow h \rightarrow WW$ (0jet)	0.20	0.19	98.2	1.8	0.0	0.0	0.0
ATL (pp) $\rightarrow h \rightarrow WW$ (1jet)	0.36	0.33	88.4	11.6	0.0	0.0	0.0
ATL (pp) $\rightarrow h \rightarrow WW$ (VBF-like)	0.21	0.12	8.1	91.9	0.0	0.0	0.0
ATL (pp) $\rightarrow h \rightarrow ZZ$ (ggF-like)	0.13	0.12	88.7	7.2	2.0	1.4	0.7
ATL (pp) $\rightarrow h \rightarrow ZZ$ (VBF-like)	0.34	0.21	44.7	53.2	0.7	0.4	1.0
ATL (pp) $\rightarrow h \rightarrow ZZ$ (VH -like)	0.32	0.13	30.1	9.0	34.8	12.1	14.0
ATL (pp) $\rightarrow h \rightarrow ZZ$ ($t\bar{t}H$ -like)	0.46	0.20	8.7	1.7	1.7	3.1	84.8
ATL (pp) $\rightarrow h \rightarrow Z\gamma$	1.47	0.57	87.6	7.1	3.1	1.7	0.6
ATL (pp) $\rightarrow h \rightarrow \mu\mu$	0.47	0.19	87.6	7.1	3.1	1.7	0.6
ATL (pp) $\rightarrow h \rightarrow \mu\mu$ ($t\bar{t}H$)	0.73	0.26	0.0	0.0	0.0	0.0	100.0
ATL (pp) $\rightarrow h \rightarrow \tau\tau$ (VBF-like)	0.22	0.19	19.8	80.2	0.0	0.0	0.0
CMS (pp) $\rightarrow h \rightarrow \gamma\gamma$	0.06	0.04	87.6	7.1	3.1	1.7	0.6
CMS (pp) $\rightarrow h \rightarrow WW$	0.06	0.04	88.1	7.1	3.1	1.7	0.0
CMS (pp) $\rightarrow h \rightarrow ZZ$	0.07	0.04	88.1	7.1	3.1	1.7	0.0
CMS (pp) $\rightarrow h \rightarrow Z\gamma$	0.62	0.20	87.6	7.1	3.1	1.7	0.6
CMS (pp) $\rightarrow h \rightarrow b\bar{b}$	0.11	0.05	0.0	0.0	57.0	32.3	10.7
CMS (pp) $\rightarrow h \rightarrow \mu\mu$	0.40	0.20	87.6	7.1	3.1	1.7	0.6
CMS (pp) $\rightarrow h \rightarrow \tau\tau$	0.08	0.05	68.6	27.7	2.4	1.4	0.0

0.21629 ± 0.00066 [73]. Following the calculations of Ref. [74], we can obtain the contributions of the charged and neutral Higgses to the tree-level couplings \bar{g}_b^L and \bar{g}_b^R , and the QCD corrections is included, whose expressions are given in Ref. [75].

The measurement uncertainties of Higgs signal rates will be sizably reduced at the LHC-300 fb $^{-1}$ and LHC-3000 fb $^{-1}$. The projected 1σ sensitivities for channels are shown in Tabel II. The sensitivities of ATLAS include the current theory systematic uncertainties, the statistical and experimental systematic uncertainties. The sensitivities of CMS correspond to Scenario 2, which extrapolates the analyses of 7 and 8 TeV data to 14 TeV assuming the theory uncertainties will be reduced by a factor of 2 while other uncertainties are reduced by a factor of $1/\sqrt{\mathcal{L}}$. Using the projected 1σ sensitivities for channels, we define

$$\chi^2 = \sum_i \frac{(\epsilon_{ggH}^i R_{ggH} + \epsilon_{VBF}^i R_{VBF} + \epsilon_{WH}^i R_{WH} + \epsilon_{ZH}^i R_{ZH} + \epsilon_{t\bar{t}H}^i R_{t\bar{t}H} - 1)^2}{\sigma_i^2}. \quad (5)$$

Where $R_j = \frac{(\sigma \times BR)_j}{(\sigma \times BR)_j^{SM}}$ with j denoting the partonic processes ggH , VBF , WH , ZH and $t\bar{t}H$. ϵ_j^i and σ_i denote the assumed signal composition of the partonic process j and 1σ uncertainty for the signal i , respectively. Thus, χ^2 is used to determine the how well 2HDMs can be distinguished from the SM by the future measurement of the 125 GeV Higgs at the LHC. In another words, we assume the future Higgs signal data have no deviation from the SM expectation, and estimate the limits on the 2HDMs using the projected 1σ uncertainties for channels at the LHC-300 fb $^{-1}$ and LHC-3000 fb $^{-1}$.

On the other hand, the design center of mass energy at the International Linear Collider (ILC) are 250 GeV and 500 GeV with a possibility to upgrade to 1 TeV. For Higgs measurements, the beam polarizations are tuned to be $(e^-, e^+) = (-0.8, +0.3)$ at 250 GeV and 500 GeV as well as $(e^-, e^+) = (-0.8, +0.2)$ at 1 TeV. At $\sqrt{s} = 250$ GeV, an absolute measurement of the production cross section can be performed from the Z Higgsstrahlung near threshold. The weak boson fusion process dominates over the Z Higgsstrahlung process at 500 GeV and 1000 GeV. The projected 1σ sensitivities of channels at the ILC are shown in Table III. Using the projected 1σ sensitivities for channels at the ILC, we define

$$\chi^2 = \sum_i \frac{(R_i - 1)^2}{\sigma_i^2}, \quad (6)$$

where R_i and σ_i represent the signal strength prediction from the 2HDMs and the 1σ uncertainty for the signal i , respectively.

TABLE III: Projected 1σ sensitivities of channels for the ILC operating at $\sqrt{s} = 250$ GeV, 500 GeV and 1000 GeV with a corresponding integrated luminosity of 250 fb^{-1} , 500 fb^{-1} and 1000 fb^{-1} , respectively [78].

Channel	250 GeV	500 GeV	1 TeV
μ_{Zh}	2.6%	3.0%	—
$\mu_{Zh}(b\bar{b})$	1.2%	1.8%	—
$\mu_{Zh}(c\bar{c})$	8.3%	13%	—
$\mu_{Zh}(gg)$	7.0%	11%	—
$\mu_{Zh}(WW)$	6.4%	9.2%	—
$\mu_{Zh}(ZZ)$	18%	25%	—
$\mu_{Zh}(\tau\tau)$	4.2%	5.4%	—
$\mu_{Zh}(\gamma\gamma)$	34%	34%	—
$\mu_{Zh}(\mu\mu)$	100%	—	—
$\mu_{WW}(b\bar{b})$	10.5%	0.7%	0.5%
$\mu_{WW}(c\bar{c})$	—	6.2%	3.1%
$\mu_{WW}(gg)$	—	4.1%	2.6%
$\mu_{WW}(WW)$	—	2.4%	1.6%
$\mu_{WW}(ZZ)$	—	8.2%	4.1%
$\mu_{WW}(\tau\tau)$	—	9.0%	3.1%
$\mu_{WW}(\gamma\gamma)$	—	23%	8.5%
$\mu_{WW}(\mu\mu)$	—	—	31%
$\mu_{t\bar{t}}(b\bar{b})$	—	28%	6.0%

In our calculations, the input parameters are taken as m_{12}^2 , $\tan\beta$, $\sin(\beta - \alpha)$ and the physical Higgs masses (m_h , m_H , m_A , m_{H^\pm}). We fix m_H as 125 GeV, and scan randomly the

parameters in the following ranges:

$$\begin{aligned}
20 \text{ GeV} \leq m_h \leq 125 \text{ GeV}, \quad 50 \text{ GeV} \leq m_A, \quad m_{H^\pm} \leq 900 \text{ GeV}, \\
-0.7 \leq \sin(\beta - \alpha) \leq 0.7, \quad 0.1 \leq \tan \beta \leq 40, \\
m_{12}^2 \text{ (GeV}^2\text{)} = \pm(0.1)^2, \pm(1)^2, \pm(5)^2, \pm(10)^2, \pm(30)^2, \pm(50)^2, \\
\pm(100)^2, \pm(180)^2, \pm(300)^2, \pm(400)^2.
\end{aligned} \tag{7}$$

IV. RESULTS AND DISCUSSIONS

In addition to that the theoretical constraints are satisfied, we require the 2HDMs to explain the experimental data of flavor observables and the electroweak precision data within 2σ range, and fit the current Higgs signal data and future LHC and ILC data at the 2σ level.

In Fig. 1, we project the surviving samples on the plane of $\sin(\beta - \alpha)$ versus $\tan \beta$. χ^2 fit to current Higgs data in the SM is marginally larger than the minimum of χ^2 in the Type-I model, and smaller than those of Type-II, Lepton-specific and Flipped models. χ^2 can be also smaller than SM value in the Next-to-Minimal Supersymmetric Standard Model [79–81], but at most approaches to SM value in the little Higgs models for very large scale f [82–84]. In the four 2HDMs, a small $\tan \beta$ is favored, and a main reason is that one of λ_1 and λ_2 is easy to become non-perturbative for the large $\tan \beta$. However, $\tan \beta$ is required to be larger than 1.6 for the Type-I and Lepton-specific models, and 1.1 for the Type-II and Flipped models. The main constraints are from Δm_{B_d} and Δm_{B_s} which are sensitive to $\cot \beta$. The Type-I model is less constrained than the other three models by the current data. $\sin(\beta - \alpha)$ is allowed to vary in the range of -0.55 and 0.56. In the Type-I model, the neutral CP-even Higgs couplings to fermions have a universal varying factor. In addition, the charged Higgs Yukawa couplings approach to zero in the large $\tan \beta$ limit, which is less constrained by $B \rightarrow X_s \gamma$ and R_b .

Fig. 1 shows that the surviving samples lie in the two different regions in the Type-II, Lepton-specific and Flipped models. In one region, the 125 GeV Higgs couplings are near the SM values, called SM-like region. In the other region, at least one of the Higgs Yukawa couplings has opposite sign to the corresponding coupling to VV, called wrong-sign Yukawa coupling region. Now we analyze the two regions in detail. In the four models, there are two factors of $\frac{\cos \alpha}{\cos \beta}$ and $\frac{\sin \alpha}{\sin \beta}$ for the heavy CP-even Higgs Yukawa couplings normalized to

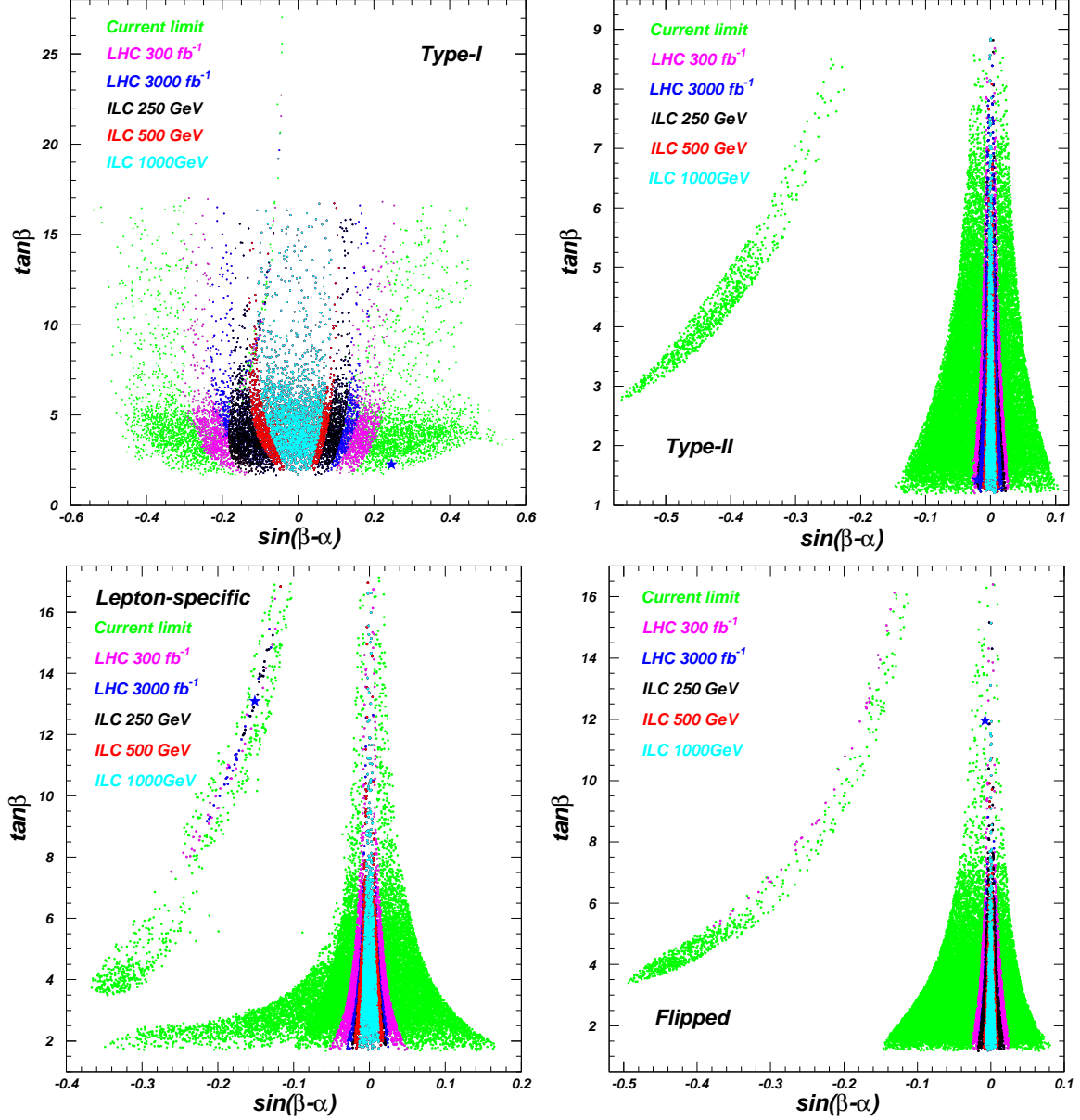


FIG. 1: The scatter plots of surviving samples projected on the planes of $\sin(\beta - \alpha)$ versus $\tan \beta$. The samples with the minimal values of χ^2 are marked out as stars.

the corresponding SM values.

For $\frac{\sin \alpha}{\sin \beta}$,

$$\frac{\sin \alpha}{\sin \beta} = \cos(\beta - \alpha) - \sin(\beta - \alpha) \cot \beta. \quad (8)$$

In the wrong-sign Yukawa coupling region where both $|\varepsilon|$ and $\sin^2(\beta - \alpha)$ are much smaller than 1,

$$\frac{\sin \alpha}{\sin \beta} = -1 + \varepsilon, \quad \cos(\beta - \alpha) \simeq 1 - \frac{1}{2} \sin^2(\beta - \alpha). \quad (9)$$

From Eqs. (8) and (9), we obtain

$$\tan \beta = \frac{2 \sin(\beta - \alpha)}{4 - 2\varepsilon - \sin^2(\beta - \alpha)}. \quad (10)$$

This implies the wrong-sign $hf\bar{f}$ coupling with a normalized factor $\frac{\sin \alpha}{\sin \beta}$ can only be achieved for $\tan \beta$ is much smaller than 1, which is excluded by the current experimental data as the above discussions.

For $\frac{\cos \alpha}{\cos \beta}$,

$$\frac{\cos \alpha}{\cos \beta} = \cos(\beta - \alpha) + \sin(\beta - \alpha) \tan \beta, \quad (11)$$

$$\frac{\cos \alpha}{\cos \beta} = \cos(\beta + \alpha) + \sin(\beta + \alpha) \tan \beta. \quad (12)$$

For $\cos(\beta - \alpha) = 1$ and $\cos(\beta + \alpha) = -1$, the $Hf\bar{f}$ couplings normalize to the SM value equal to 1 and -1, which are the limiting cases of the SM-like region and the wrong-sign Yukawa coupling region, respectively.

In the wrong-sign Yukawa coupling region where both $|\varepsilon|$ and $\sin^2(\beta - \alpha)$ are much smaller than 1,

$$\frac{\cos \alpha}{\cos \beta} = -1 + \varepsilon, \quad \cos(\beta - \alpha) \simeq 1 - \frac{1}{2} \sin(\beta - \alpha)^2. \quad (13)$$

From Eqs. (11) and (13), we obtain

$$\tan \beta = \frac{\frac{1}{2} \sin(\beta - \alpha)^2 + \varepsilon - 2}{\sin(\beta - \alpha)}, \quad (14)$$

$$\sin(\beta - \alpha) = \frac{\frac{1}{2} \sin(\beta - \alpha)^2 + \varepsilon - 2}{\tan \beta}. \quad (15)$$

From Eq. (14), the wrong-sign $hf\bar{f}$ coupling with a normalized factor $\frac{\cos \alpha}{\cos \beta}$ can only be achieved for $\tan \beta$ is much larger than 1 and $\sin(\beta - \alpha) < 0$.

In the SM-like region,

$$\frac{\cos \alpha}{\cos \beta} = 1 - \varepsilon, \quad \cos(\beta - \alpha) \simeq 1 - \frac{1}{2} \sin(\beta - \alpha)^2. \quad (16)$$

From Eqs. (11) and (16), we obtain

$$\tan \beta = \frac{\frac{1}{2} \sin(\beta - \alpha)^2 - \varepsilon}{\sin(\beta - \alpha)}, \quad (17)$$

$$\sin(\beta - \alpha) = \frac{\frac{1}{2} \sin(\beta - \alpha)^2 - \varepsilon}{\tan \beta}. \quad (18)$$

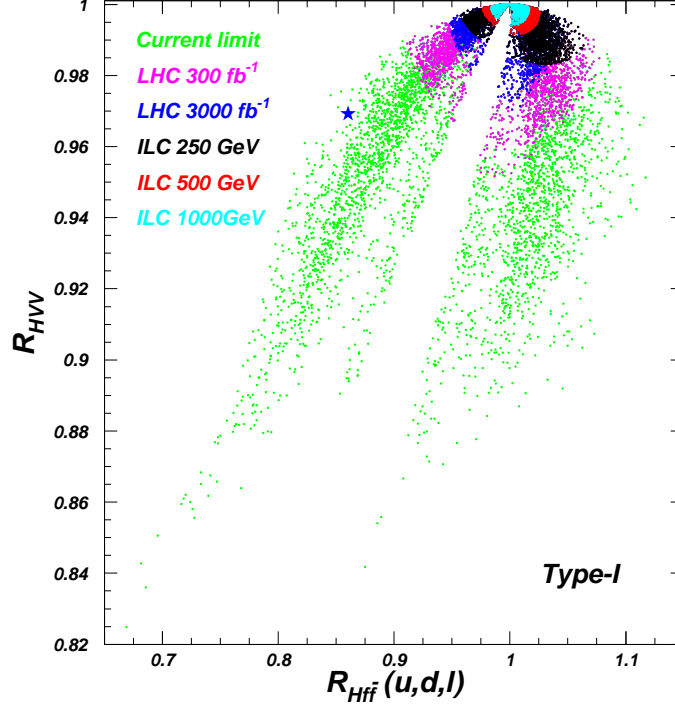


FIG. 2: The scatter plots of surviving samples in the Type-I model projected on the planes of $R_{Hf\bar{f}}(u,d,l)$ versus R_{HVV} . Where $R_{Hf\bar{f}}$ and R_{HVV} denote the heavy CP-even Higgs couplings to $f\bar{f}$ and VV normalized to the corresponding SM values.

Compared Eqs. (14) and (17), the lower bound of $\tan\beta$ in the wrong-sign Yukawa coupling region should be larger than that in the SM-like region. Compared Eq. (15) and (18), the absolute value of $\sin(\beta - \alpha)$ in the wrong-sign Yukawa coupling region should be larger than that in the SM-like region for the same $\tan\beta$. Recently, Ref. [28] discusses the wrong-sign Yukawa coupling of the light CP-even Higgs in the Type-II model in detail.

Therefore, the wrong-sign Yukawa coupling can be achieved for the $hdd\bar{d}$ and $hl\bar{l}$ couplings in the Type-II model, $hl\bar{l}$ in the Lepton-specific model, and $hdd\bar{d}$ in the Flipped model. The above analyses are confirmed by what are shown in the Fig. 1. In the wrong-sign Yukawa coupling regions, the current data require $\tan\beta > 2.7$ for the Type-II model, $\tan\beta > 3.5$ for the Lepton-specific model and $\tan\beta > 3.4$ for the Flipped model. $\sin(\beta - \alpha)$ is allowed to be as low as -0.57 for the Type-II model, -0.37 for the Lepton-specific model and -0.49 for the Flipped model. In the SM-like regions, the current data require $-0.15 < \sin(\beta - \alpha) < 0.11$ for the Type-II model, $-0.35 < \sin(\beta - \alpha) < 0.17$ for the Lepton-specific model and $-0.15 < \sin(\beta - \alpha) < 0.08$ for the Flipped model.

For the Type-I model, the LHC-300 fb^{-1} , LHC-3000 fb^{-1} , ILC-250 GeV, ILC-500 GeV

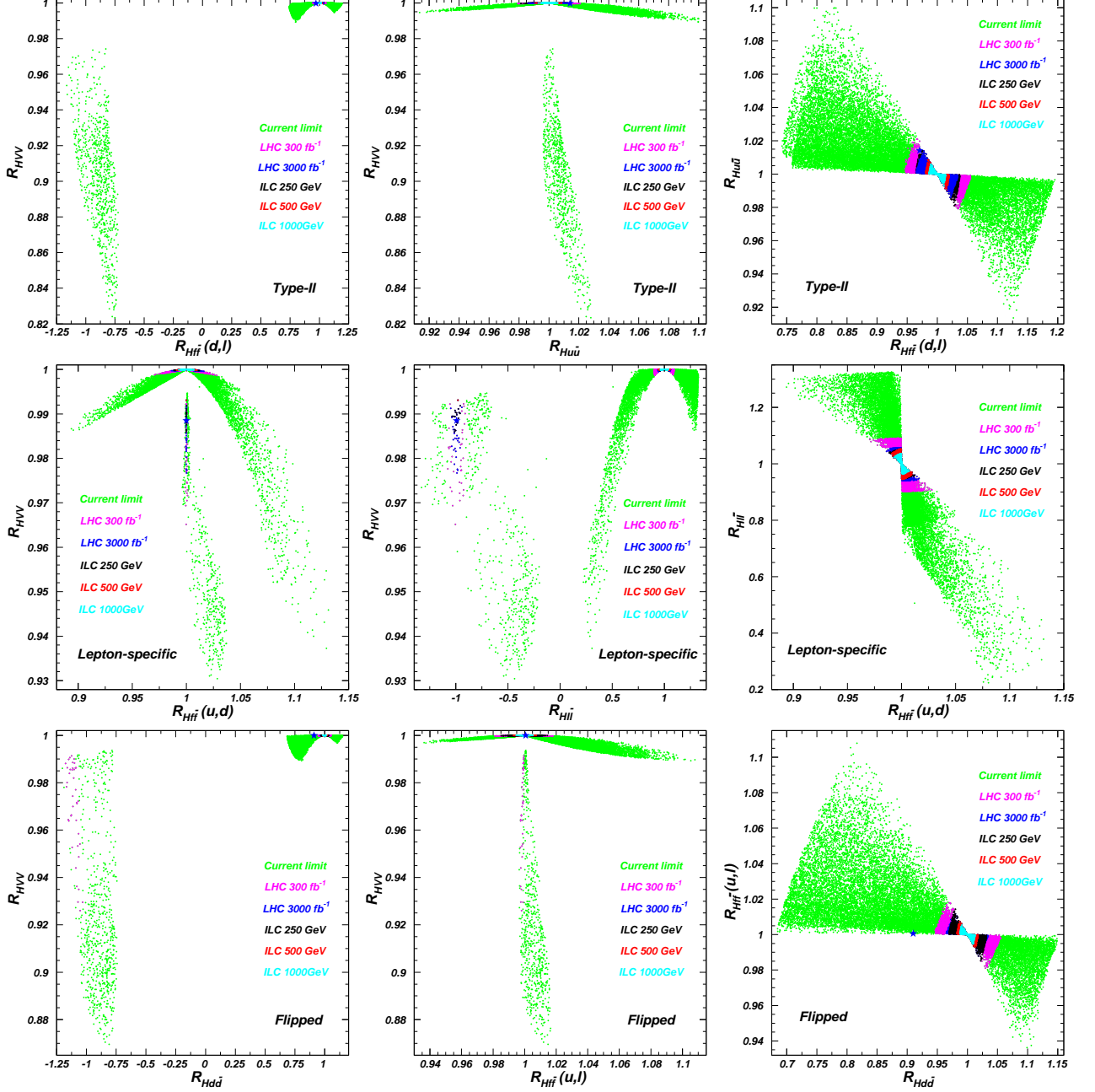


FIG. 3: Same as Fig. 2, but for the Type-II, Lepton-specific and Flipped models.

and ILC-1000 GeV will gradually narrow the allowed ranges of $\sin(\beta - \alpha)$. For the Type-II and Flipped models, the LHC-300 fb^{-1} can narrow the ranges of $\sin(\beta - \alpha)$ sizably, and the ILC-250 GeV can not narrow the ranges of $\sin(\beta - \alpha)$ more visibly than LHC-3000 fb^{-1} .

In Fig. 2 and Fig. 3, we project the surviving samples on the planes of the 125 GeV Higgs couplings. From Fig. 2, for the Type-I model, we find that the allowed ranges of HVV and $Hf\bar{f}$ couplings are $0.825 \sim 1.0$ and $0.669 \sim 1.117$ for the current constraints, $0.952 \sim 1.0$

and $0.911 \sim 1.075$ for the LHC-300 fb $^{-1}$, $0.97 \sim 1.0$ and $0.948 \sim 1.048$ for the LHC-3000 fb $^{-1}$, $0.983 \sim 1.0$ and $0.957 \sim 1.063$ for the ILC-250 GeV, $0.991 \sim 1.0$ and $0.977 \sim 1.026$ for the ILC-500 GeV as well as $0.994 \sim 1.0$ and $0.984 \sim 1.017$ for the ILC-1000 GeV.

For the Type-II model, in the wrong-sign $Hd\bar{d}$ and $Hl\bar{l}$ couplings region, the current data require $0.825 < R_{HVV} < 0.975$, $-1.17 < R_{Hd\bar{d}} (R_{Hl\bar{l}}) < -0.72$ and $0.996 < R_{Hu\bar{u}} < 1.028$. The LHC-300 fb $^{-1}$ can exclude the wrong-sign $Hd\bar{d}$ and $Hl\bar{l}$ couplings region at the 2σ level. In the SM-like region, the current data require $0.989 < R_{HVV} < 1.0$, $0.74 < R_{Hd\bar{d}} (R_{Hl\bar{l}}) < 1.2$ and $0.913 < R_{Hu\bar{u}} < 1.1$. The future LHC and ILC will require R_{HVV} to be very close to 1. The allowed ranges of $R_{Hd\bar{d}} (R_{Hl\bar{l}})$ and $R_{Hu\bar{u}}$ are $0.946 \sim 1.055$ and $0.979 \sim 1.021$ for the LHC-300 fb $^{-1}$, $0.965 \sim 1.034$ and $0.986 \sim 1.014$ for the LHC-3000 fb $^{-1}$, $0.965 \sim 1.038$ and $0.981 \sim 1.015$ for the ILC-250 GeV, $0.981 \sim 1.019$ and $0.99 \sim 1.009$ for the ILC-500 GeV as well as $0.986 \sim 1.014$ and $0.993 \sim 1.006$ for the ILC-1000 GeV.

For the Lepton-specific model, in the wrong-sign $Hl\bar{l}$ coupling region, the current data require $0.93 < R_{HVV} < 0.995$, $-1.33 < R_{Hl\bar{l}} < -0.226$ and $0.996 < R_{Hu\bar{u}} (R_{Hd\bar{d}}) < 1.037$. The LHC-300 fb $^{-1}$, LHC-3000 fb $^{-1}$, ILC-250 GeV and ILC-500 GeV can gradually constrain the absolute of Higgs couplings to $f\bar{f}$ and VV to be close to SM values in the wrong-sign $Hl\bar{l}$ coupling region, and the ILC-1000 GeV can exclude the whole wrong-sign $Hl\bar{l}$ coupling region at the 2σ level. In the SM-like region, the current data require $0.937 < R_{HVV} < 1.0$, $0.224 < R_{Hl\bar{l}} < 1.325$ and $0.893 < R_{Hu\bar{u}} (R_{Hd\bar{d}}) < 1.132$. The future LHC-300 fb $^{-1}$ will require R_{HVV} to be in the range of 0.998 and 1.0. The other future LHC and ILC experiments will require R_{HVV} to be very close to 1. The allowed ranges of $R_{Hu\bar{u}} (R_{Hd\bar{d}})$ and $R_{Hl\bar{l}}$ are $0.971 \sim 1.028$ and $0.901 \sim 1.091$ for the LHC-300 fb $^{-1}$, $0.986 \sim 1.016$ and $0.94 \sim 1.058$ for the LHC-3000 fb $^{-1}$, $0.988 \sim 1.013$ and $0.946 \sim 1.051$ for the ILC-250 GeV, $0.991 \sim 1.01$ and $0.945 \sim 1.053$ for the ILC-500 GeV as well as $0.993 \sim 1.007$ and $0.963 \sim 1.037$ for the ILC-1000 GeV.

For the Flipped model, in the wrong-sign $Hd\bar{d}$ coupling region, the current data require $0.87 < R_{HVV} < 0.994$, $-1.2 < R_{Hd\bar{d}} < -0.74$ and $0.996 < R_{Hu\bar{u}} (R_{Hl\bar{l}}) < 1.017$. The LHC-300 fb $^{-1}$ can exclude some samples with $R_{Hd\bar{d}} < -1$ and $R_{Hu\bar{u}}$ very close to 1. Both the LHC-3000 fb $^{-1}$ and ILC-250 GeV can exclude the whole wrong-sign $Hd\bar{d}$ coupling region at the 2σ level. In the SM-like region, the current data require $0.989 < R_{HVV} < 1.0$, $0.682 < R_{Hd\bar{d}} < 1.152$ and $0.935 < R_{Hu\bar{u}} (R_{Hl\bar{l}}) < 1.108$. The future LHC and ILC will require the R_{HVV} to be very close to 1. The allowed ranges of $R_{Hd\bar{d}}$ and $R_{Hu\bar{u}} (R_{Hl\bar{l}})$ are

0.946 \sim 1.056 and 0.981 \sim 1.018 for the LHC-300 fb $^{-1}$, 0.965 \sim 1.034 and 0.988 \sim 1.012 for the LHC-3000 fb $^{-1}$, 0.97 \sim 1.032 and 0.985 \sim 1.015 for the ILC-250 GeV, 0.983 \sim 1.018 and 0.993 \sim 1.008 for the ILC-500 GeV as well as 0.987 \sim 1.013 and 0.994 \sim 1.006 for the ILC-1000 GeV.

V. CONCLUSION

In this paper, we assume the 125 GeV Higgs discovered at the LHC is the heavy CP-even Higgs of the Type-I, Type-II, Lepton-specific and Flipped 2HDMs, and examine the parameter space allowed by the latest Higgs signal data, the non-observation of additional Higgs at the collider, and the theoretical constraints from vacuum stability, unitarity and perturbativity as well as the experimental constraints from the electroweak precision data and flavor observables. We obtain the following observations:

(i) The current experiment data favor a small $\tan\beta$, but give a lower limit of $\tan\beta$, $\tan\beta > 1.6$ for the Type-I model, $\tan\beta > 1.1$ (2.7) for the SM-like region (wrong-sign Yukawa coupling region) of the Type-II model, $\tan\beta > 1.6$ (3.5) for the SM-like region (wrong-sign Yukawa coupling region) of the Lepton-specific model, and $\tan\beta > 1.1$ (3.4) for the SM-like region (wrong-sign Yukawa coupling region) of the Flipped model.

(ii) For the Type-I model, the current experimental data require $0.825 < HVV < 1.0$ and $0.669 < Hf\bar{f} (u, d, l) < 1.117$.

(iii) For the Type-II model, the current experimental data require $0.825 < R_{HVV} < 0.975$, $-1.17 < R_{Hd\bar{d}} (R_{H\bar{u}}) < -0.72$ and $0.996 < R_{Hu\bar{u}} < 1.028$ in the wrong-sign $Hd\bar{d}$ and $H\bar{u}\bar{l}$ couplings region, and $0.989 < R_{HVV} < 1.0$, $0.74 < R_{Hd\bar{d}} (R_{H\bar{u}}) < 1.2$ and $0.913 < R_{Hu\bar{u}} < 1.1$ in the SM-like region.

(iv) For the Lepton-specific model, the current experimental data require $0.93 < R_{HVV} < 0.995$, $-1.33 < R_{H\bar{u}} < -0.226$ and $0.996 < R_{Hu\bar{u}} (R_{Hd\bar{d}}) < 1.037$ in the wrong-sign $H\bar{u}\bar{l}$ coupling region, and $0.937 < R_{HVV} < 1.0$, $0.224 < R_{H\bar{u}} < 1.325$ and $0.893 < R_{Hu\bar{u}} (R_{Hd\bar{d}}) < 1.132$ in the SM-like region.

(v) For the Flipped model, the current experimental data require $0.87 < R_{HVV} < 0.994$, $-1.2 < R_{Hd\bar{d}} < -0.74$ and $0.996 < R_{Hu\bar{u}} (R_{H\bar{u}}) < 1.017$ in the wrong-sign $Hd\bar{d}$ coupling region, and $0.989 < R_{HVV} < 1.0$, $0.682 < R_{Hd\bar{d}} < 1.152$ and $0.935 < R_{Hu\bar{u}} (R_{H\bar{u}}) < 1.108$ in the SM-like region.

Further, we give the projected limits on $\tan\beta$, $\sin(\beta - \alpha)$, $Hf\bar{f}$ and HVV couplings from the future measurements of the 125 GeV Higgs at the LHC and ILC, including the LHC-300 fb⁻¹, LHC-3000 fb⁻¹ as well as the ILC-250 GeV, ILC-500 GeV and ILC-1000 GeV. Assuming that the future Higgs signal data have no deviation from the SM expectation, the LHC-300 fb⁻¹, LHC-3000 fb⁻¹ and ILC-1000 GeV can exclude the wrong-sign Yukawa coupling regions of the Type-II, Flipped and Lepton-specific models at the 2σ level, respectively. The future experiments at the LHC and ILC will constrain the Higgs couplings to be very close to SM values, especially for the HVV coupling.

Acknowledgment

This work was supported by the National Natural Science Foundation of China (NNSFC) under grant No. 11105116.

-
- [1] S. Chatrchyan et al. [CMS Collaboration], Phys. Lett. B **716**, 30 (2012).
 - [2] G. Aad et al. [ATLAS Collaboration], Phys. Lett. B **716**, 1 (2012).
 - [3] T. Aaltonen *et al.* [CDF and D0 Collaborations], Phys. Rev. D **88**, 052014 (2013).
 - [4] H. E. Haber, G. L. Kane and T. Sterling, Nucl. Phys. B **161**, 493 (1979).
 - [5] L. J. Hall and M. B. Wise, Nucl. Phys. B **187**, 397 (1981).
 - [6] J. F. Donoghue and L. F. Li, Phys. Rev. D **19**, 945 (1979).
 - [7] V. D. Barger, J. L. Hewett and R. J. N. Phillips, Phys. Rev. D **41**, 3421 (1990).
 - [8] Y. Grossman, Nucl. Phys. B **426**, 3 (1994).
 - [9] A. G. Akeroyd and W. J. Stirling, Nucl. Phys. B **447**, 3 (1995).
 - [10] A. G. Akeroyd, Phys. Lett. B **377**, 95 (1996).
 - [11] A. G. Akeroyd, J. Phys. G **24**, 1983 (1998).
 - [12] M. Aoki, S. Kanemura, K. Tsumura and K. Yagyu, Phys. Rev. D **80**, 015017 (2009).
 - [13] A. Pich, P. Tuzon, Phys. Rev. D **80**, 091702 (2009).
 - [14] C.-Y. Chen and S. Dawson, Phys. Rev. D **87**, 055016 (2013).
 - [15] B. Grinstein and P. Uttayarat, JHEP **1306**, 094 (2013) [Erratum-ibid. 1309, 110 (2013)].
 - [16] B. Coleppa, F. Kling, S. Su, JHEP **1401**, 161 (2014).

- [17] O. Eberhardt, U. Nierste, M. Wiebusch, JHEP **07**, 118 (2013).
- [18] C. -W. Chiang and K. Yagyu, JHEP **1307**, 160 (2013).
- [19] B. Grinstein and P. Uttayarat, JHEP **1306**, 094 (2013).
- [20] C.-Y. Chen, S. Dawson and M. Sher, Phys. Rev. D **88**, 015018 (2013).
- [21] N. Craig, J. Galloway and S. Thomas, arXiv:1305.2424.
- [22] G. Belanger, B. Dumont, U. Ellwanger, J. F. Gunion and S. Kraml, Phys. Rev. D **88**, 075008 (2013).
- [23] D. Lopez-Val, T. Plehn and M. Rauch, JHEP **1310**, 134 (2013).
- [24] S. Choi, S. Jung and P. Ko, JHEP **1310**, 225 (2013).
- [25] S. Chang, S. K. Kang, J. -P. Lee, K. Y. Lee, S. C. Park and J. Song, arXiv:1310.3374.
- [26] V. Barger, L. L. Everett, H. E. Logan and G. Shaughnessy, Phys. Rev. D **88**, 115003 (2013).
- [27] C.-Y. Chen, arXi:1308.3487.
- [28] P. M. Ferreira, R. Santos, J. F. Gunion, H. E. Haber, arXiv:1403.4736.
- [29] J. Baglio, O. Eberhardt, U. Nierste, M. Wiebusch, arXiv:1403.1264.
- [30] W. Altmannshofer, S. Gori and G. D. Kribs, Phys. Rev. D **86**, 115009 (2012).
- [31] Y. Bai, V. Barger, L. L. Everett and G. Shaughnessy, Phys. Rev. D **87**, 115013 (2013).
- [32] K. Cheung, J. S. Lee, P.-Y. Tseng, JHEP **1401**, 085 (2014).
- [33] A. Celis, V. Ilisie, A. Pich, JHEP **1307**, 053 (2013).
- [34] A. Celis, V. Ilisie, A. Pich, JHEP **1312**, 095 (2013).
- [35] W. Altmannshofer, S. Gori, G. D. Kribs, Phys. Rev. D **86**, 115009 (2012).
- [36] L. Wang, X.-F. Han, JHEP **1404**, 128 (2014).
- [37] R. A. Battye, G. D. Brawn, A. Pilaftsis, JHEP **1108**, 020 (2011).
- [38] P. Bechtle, S. Heinemeyer, O. Stål, T. Stefaniak, G. Weiglein, Eur. Phys. Jour. C **74**, 2711 (2014).
- [39] ATLAS Collaboration, ATLAS-CONF-2013-030, ATLAS-COM-CONF-2013-028.
- [40] G. Aad *et al.* [ATLAS Collaboration], Phys. Lett. B **726**, 88-119 (2013).
- [41] ATLAS Collaboration, ATLAS-CONF-2013-013, ATLAS-COM-CONF-2013-018.
- [42] ATLAS Collaboration, ATLAS-CONF-2012-091, ATLAS-COM-CONF-2012-109.
- [43] ATLAS Collaboration, ATLAS-CONF-2013-012, ATLAS-COM-CONF-2013-015.
- [44] ATLAS collaboration, ATLAS-CONF-2013-079, ATLAS-COM-CONF-2013-080.
- [45] ATLAS collaboration, ATLAS-CONF-2013-075, ATLAS-COM-CONF-2013-069.

- [46] ATLAS collaboration ATLAS-CONF-2013-108, ATLAS-COM-CONF-2013-095.
- [47] CMS Collaboration, CMS-PAS-HIG-13-001.
- [48] CMS Collaboration, CMS-PAS-HIG-13-004. Updated results (dated Dec 2013) taken from TWiki page: <https://twiki.cern.ch/twiki/bin/view/CMSPublic/Hig13004TWikiUpdate>.
- [49] S. Chatrchyan et al. [CMS Collaboration], arXiv:1401.5041.
- [50] CMS Collaboration, CMS-PAS-HIG-13-020.
- [51] CMS Collaboration, CMS-PAS-HIG-13-019.
- [52] CMS Collaboration, CMS-PAS-HIG-13-015.
- [53] CMS Collaboration, CMS-PAS-HIG-12-015.
- [54] S. Chatrchyan et al. [CMS Collaboration], JHEP **1401**, 096 (2014).
- [55] CMS Collaboration, CMS-PAS-HIG-13-017.
- [56] CMS Collaboration, CMS-PAS-HIG-13-002.
- [57] CMS Collaboration, CMS-PAS-HIG-13-007.
- [58] CMS Collaboration, CMS-PAS-HIG-13-012.
- [59] T. Aaltonen *et al.* [CDF Collaboration], Phys. Rev. D **88**, 052013 (2013).
- [60] V. M. Abazov *et al.* [D0 Collaboration], Phys. Rev. D **88**, 052011 (2013).
- [61] P. Bechtle, S. Heinemeyer, O. Stål, T. Stefaniak, G. Weiglein, arXiv:1403.1582.
- [62] D. Eriksson, J. Rathsmann, O. Stål, Comput. Phys. Commun. **181**, 189-205 (2010); Comput. Phys. Commun. **181**, 833-834 (2010).
- [63] J. Beringer *et al.* (Particle Data Group), Phys. Rev. D **86**, 010001 (2012).
- [64] F. Mahmoudi, Comput. Phys. Commun. **180**, 1579-1673 (2009).
- [65] Y. Amhis *et al.* [Heavy Flavor Averaging Group], arXiv:1207.1158.
- [66] R. Aaij *et al.* [LHCb Collaboration], Phys. Rev. Lett. **110**, 021801 (2013).
- [67] <http://www.slac.stanford.edu/xorg/hfag/rare/2013/radll/index.html>
- [68] P. Bechtle, O. Brein, S. Heinemeyer, G. Weiglein, K. E. Williams, Comput. Phys. Commun. **181**, 138-167 (2010).
- [69] P. Bechtle, O. Brein, S. Heinemeyer, O. Stål, T. Stefaniak, G. Weiglein, K. E. Williams, Eur. Phys. Jour. C **74**, 2693 (2014).
- [70] Particle Data Group, 2013 partial update for the 2014 edition.
- [71] C. Q. Geng and J. N. Ng, Phys. Rev. D **38**, 2857 (1988) [Erratum-ibid. D 41, 1715 (1990)].
- [72] A. Freitas and Y.-C. Huang, JHEP **1208**, 050 (2012) [Erratum-ibid. 1305, 074 (2013)]

- [Erratum-ibid. 1310, 044 (2013)].
- [73] K. Nakamura et al. [Particle Data Group], J. Phys. G **37**, 075021 (2010).
 - [74] H. E. Haber, H. E. Logan, Phys. Rev. D **62**, 015011 (2000).
 - [75] G. Degrossi, P. Slavich, Phys. Rev. D **81**, 075001 (2010).
 - [76] ATLAS Collaboration, ATL-PHYS-PUB-2013-014.
 - [77] CMS Collaboration, arXiv:1307.7135.
 - [78] D.M. Asner1 *et al.*, arXiv:1310.0763.
 - [79] J. Cao, Z. Heng, J. M. Yang, J. Zhu, JHEP **1210**, 079 (2012).
 - [80] J.-J. Cao, Z.-X. Heng, J. M. Yang, Y.-M. Zhang, J.-Y. Zhu, JHEP **1203**, 086 (2012).
 - [81] J. F. Gunion, Y. Jiang, S. Kraml, Phys. Lett. B **710**, 454-459 (2012).
 - [82] L. Wang, J. M. Yang, J. Zhu, Phys. Rev. D **88**, 075018 (2013).
 - [83] X.-F. Han, L. Wang, J. M. Yang, J. Zhu, Phys. Rev. D **87**, 055004 (2013).
 - [84] J. Reuter, M. Tonini, JHEP **0213**, 077 (2013).